Available online at www.sciencedirect.com
ScienceDirect
Journal of Magnetic Resonance 185 (2007) 300–307
JMR Journal of Magnetic Resonance
www.elsevier.com/locate/jmr

Exploring the surface permeability of nanoporous particles by pulsed field gradient NMR

M. Krutyeva [a,*], X. Yang [b], S. Vasenkov [c], J. Kärger [a]

[a] Department of Interface Physics, University of Leipzig, Linnéstrasse 5, D-04103 Leipzig, Germany
[b] Institute of Physical Chemistry and Electrochemistry, University of Hanover, Callinstraße 3-3A, D-30167 Hanover, Germany
[c] University of Florida, Department of Chemical Engineering, Gainesville, USA

Received 6 November 2006; revised 8 January 2007
Available online 12 January 2007

Abstract

A new method to determine the surface permeability of nanoporous particles is proposed. It is based on the comparison of experimental data on tracer exchange and intracrystalline molecular mean square displacements as obtained by the PFG NMR tracer desorption technique with the corresponding solutions of the diffusion equation via dynamical Monte Carlo simulations. The method is found to be particularly sensitive in the "intermediate" regime, when the influence of intracrystalline diffusion and surface resistances of the nanoporous crystal on molecular transport are comparable and the conventional method fails. As an example, the surface permeabilities of two samples of zeolite NaCaA with different crystal sizes are determined with methane, as a probe molecule, at room temperature.

Keywords: Zeolites; Surface barriers; NMR; Permeability; Simulations

1. Introduction

Numerous technological processes in the industry of mass separation and conversion are based on the application of nanoporous materials, in particular of zeolites [1], as molecular sieves [2] and catalysts [3], respectively. In many cases, the performance of these processes is determined by the rate of molecular exchange between the nanoporous particles (the zeolite crystallites) and their surroundings. Pulsed field gradient NMR (often also referred to as pulsed gradient spin echo (PGSE) NMR) has proven to be an invaluable tool for exploring the intrinsic transport properties of such systems [4,5].

Representing the probability distribution of molecular displacements as a function of the time, the "propagator" representation [6] provides a straightforward means to discriminate between the rate of mass transfer within the crystallites ("*intracrystalline*" diffusion) and through the crystallite assemblages ("*long-range*" diffusion, sometimes referred to as "*intraparticle*" diffusion if the individual crystallites are compacted—often by means of some binder—to catalyst/adsorbent particles [7]). The coefficient of long-range diffusion may be shown [8,9] to result as the product of the relative amount of molecules in the intercrystalline space and their diffusivity. Under the precondition that the long-range diffusivity notably exceeds the intracrystalline diffusivity, the propagator may easily be separated into two constituents: a narrow one representing the displacements of those molecules which, after the given observation time t, have not yet left their crystallites, and a broad one (notably exceeding the crystal size) which is brought about by those molecules which, during t, have left the crystallites where they have resided at the beginning. The relative intensities of these two constituents (i.e. their space integrals) are directly proportional to the corresponding numbers of molecules. This means in particular that, on varying the observation time t of the PFG NMR experiment, the respective relative intensities of the broad constituent represents nothing else than the values of the tracer exchange

* Corresponding author. Fax: +49 341 97 32549.
E-mail address: krutyeva@physik.uni-leipzig.de (M. Krutyeva).

1090-7807/$ - see front matter © 2007 Elsevier Inc. All rights reserved.
doi:10.1016/j.jmr.2007.01.006

curve $\gamma(t)$ for the considered observation times [10,11]. Tracer exchange curves represent the relative amount of labelled molecules which, having been initially inside the crystallites, are, after time t, found outside in the initially unlabelled surroundings. In contrast to the conventional way of attaining tracer exchange curves by applying, e.g., isotopes [12], the "NMR" tracer desorption technique operates in milliseconds till seconds. In [13] this option has for the first time been used to estimate the intensity of transport resistances on the surface of the individual crystallites ("surface barriers"). This estimate is based on the fact that exchange curves $\gamma(t)$ are most conveniently analysed in terms of the first statistical moment [14]

$$\tau_{ex} = \int_{t=0}^{\infty} (1 - \gamma(t))\mathrm{d}t \tag{1}$$

which is easily rationalized as the time constant of molecular exchange, i.e. the mean life time of a molecule in the interior of a given crystallite. As a particular advantage of the moments method [9,14–16], the resulting first moment may be shown to be simply the sum of the first moment of each process possibly contributing to the overall behaviour. Since exchange curves are known to be rather insensitive to the particle shape, for simplifying the further analysis the crystallites are assumed to be spheres of radius R. Then, solution of the respective equations of mass transport [9,14–16] yields the simple relation:

$$\tau_{ex} = \frac{R^2}{15D_0} + \frac{R}{3\alpha} \tag{2}$$

where D_0 denotes the intracrystalline diffusivity and α stands for the permeability of the crystal surface, the reciprocal value of which is a measure of the intensity of the surface barrier. The surface permeability is defined by the relation [17–19]:

$$j = \alpha(C_{surf} - C_0) \tag{3}$$

where j is the flux density through the crystal surface, C_0 the concentration in the crystal which would be established in equilibrium with the surrounding atmosphere and C_{surf} the actual concentration close to surface.

The intracrystalline diffusivity may be directly determined by PFG NMR with sufficiently small observation times, so that any disturbance by surface effects may be estimated [20] by application of the Mitra–Sen formalism [21] or neglected at all. Hence, with the determined value of D_0 and the mean life time τ_{ex} resulting from the NMR tracer desorption curve via Eqs. (1) and (2) may be rearranged to yield, for a given value of R, the surface permeability.

Obviously, this way of analysis is trustworthy if the second term on the right-hand side of Eq. (2) turns out to notably exceed the first one, namely, for barrier-controlled molecular exchange. As soon, however, as both contributions are comparable (or, even worse, for molecular exchange controlled by intracrystalline diffusion) one has to take into consideration that uncertainties of a factor of two for both τ_{ex} (variation of the observation time often fails to cover the total range of integration in Eq. (1)) and $R^2/15D_0$ (due to dispersion in the crystal size) are not unlikely, so that the second term of the right-hand side of Eq. (2) may turn out to be the difference between two equally large quantities with a big uncertainty. Such a situation would notably complicate if not even prevent to determine the surface permeability in the conventional manner. In the present communication we present a novel option to quantitate surface resistances by means of PFG NMR which is particularly sensitive under such conditions, where intracrystalline diffusion and surface resistance are of comparable influence on the overall transport behaviour, i.e. if the two terms on the right-hand side of Eq. (2) are of equal order.

2. Conception and simulation

The conventional way of estimating surface permeabilities by means of the PFG NMR technique has been sketched in Section 1. It is based on a comparison of the rate of molecular exchange between the intra- and intercrystalline space in an "NMR tracer desorption experiment" [10] with the genuine intracrystalline diffusivities. Surface resistances, i.e. the reciprocal values of the surface permeability, are obviously the larger, the more the experimentally observed exchange rates are exceeded by their estimates solely based on the intracrystalline diffusivities.

In the present communication we follow another correlation. We investigate the interdependence between the relative amount of molecules $\gamma(t)$ that during the time interval t have left their crystallites, and the mean square displacement $\langle r^2(t)\rangle$ of the molecules that have remained within the crystallites during this very time interval. For this purpose, we consider a time interval t during which a fixed fraction of the molecules, e.g. 50% (which means $\gamma(t) = 0.5$), have left their crystallites. The mean square displacement of the molecules remaining in the crystal may obviously be expected to be the larger, the larger are the surface resistances they have to overcome on leaving the crystallites. This is intuitively anticipated by realising that, in comparison with an infinitely extended crystallite, the mean square displacement in a finite crystallite is the more reduced, the more frequently the diffusing molecules are reflected by the crystallite surface as a consequence of a reduced surface permeability. We may expect therefore that, for a given relative amount γ of molecules having exchanged with the surroundings, the mean square displacement of those still residing in one and the same crystallite is the smaller the larger are the transport barriers on the crystal surface.

The quantitation of this correlation may, in principle, be based on the solution of the diffusion equation with the relevant boundary conditions. The quantity directly accessible by the PFG NMR experiments, the mean square displacement, results from twofold integration over space, namely over all possible starting and final points of the molecular trajectories. Thus it is inherent to the considered type of

PFG NMR experiment that the solution of the diffusion equation has to be provided for any possible starting point within the crystals. Complications possibly arising from such a situation may be avoided by numerical considerations based on dynamic Monte Carlo simulations which we have used in the present study. Our estimates are based on simulations in a three-dimensional square lattice. It shall be demonstrated that extension to different shapes of the particle (spherical and cubic) does not significantly affect the obtained correlations.

In the simulations, we operate with the unit step length a and the unit time τ between two subsequent steps on a cubic lattice of sites of extension $La \times La \times La$. Each (of the six possible) step directions is selected with equal probability. Without the confinement by the lattice boundary, i.e. for either lattice sizes L sufficiently large or step numbers $n = t/\tau$ sufficiently small, the mean square displacement follows the Einstein relation

$$\langle r^2(t)\rangle = 6D_0 t \tag{4}$$

with the self-diffusivity $D_0 = a^2/(6\tau)$. Also for diffusants on boundary sites all six step directions are selected with equal probability. If, however, the step direction has been chosen to lead out of the lattice (i.e. out of the crystal), this step is only performed with probability p. Otherwise, i.e. with probability $1 - p$, the diffusant remains on the given site over a further time interval τ.

For correlating this probability p with the surface permeability as introduced by Eq. (3) one has to realize that tracer exchange experiments follow the desorption behaviour of molecules initially located in an arbitrarily selected crystal. The probability that a molecule after desorption will again enter this initial crystal is assumed to be negligibly small. In the PFG NMR experiment this situation is ensured by the requirement that the long-range diffusivity significantly exceeds the intracrystalline diffusivity. Therefore, with Eq. (3), the flux j of molecules out of the crystal is simply equal to the product αC_{surf} of surface permeability and concentration. Within our model, and using Fick's first law, this flux may also be easily represented by the relation

$$j = pD_0 \frac{C_{\mathrm{surf}}}{a} \tag{5}$$

where C_{surf}/a represents the concentration gradient between inside the crystal and outside (resulting from the respective concentrations C_{surf} and 0 at distance a), and the diffusivity is reduced by an additional factor p since jump rates out of the lattice are reduced by this very factor in comparison with those within the lattice. Equating Eqs. (3) and (5) (with $C_0 = 0$), we thus obtain

$$\alpha = \frac{pD_0}{a} \tag{6}$$

We should recollect that we have chosen the dynamic Monte Carlo simulations as a convenient way to solve the corresponding diffusion equation, including the options of an easy variation of the boundary conditions with respect to their geometry and nature. This means, however, that the introduced step length a is of no physical relevance at all. As a consequence, variation of the step length a must not affect the results of our simulations with respect to the relevant physical quantities, namely the (self-)diffusivity D and the surface permeability α. In view of Eq. (6) this means in particular, that within our model a variation of the step length a has to be associated with the corresponding change in the jump probability p out of the lattice. This requirement of self-consistency shall be shown to be fulfilled in our simulations.

The quantities determined in our simulations are the relative numbers of molecules $N_{\mathrm{rem}}(t)/N_0$ still remaining inside the crystal after a time interval t ($\equiv 1 - \gamma(t)$, with $\gamma(t)$ denoting the above introduced tracer desorption curve $\gamma(t)$) and their normalized effective diffusivity $D(t)/D_0$, which, via Eq. (4), coincides with the ratio between the mean square displacement of those molecules that are still within the crystal, $\langle r^2(t)$, and the mean square displacement that they would experience in an infinitely extended crystal, $6D_0 t$.

In a typical PFG NMR experiment, under the conditions of gas phase adsorption, the molecules are evenly distributed over the crystallites, while their concentration is negligibly small in the gas phase. Hence, the determination of $\langle r^2(t)\rangle$ via the diffusion equation implies its solution with each point within the crystal chosen as the location of its initial concentration and subsequent integration over all starting points. In analogy to Eq. (4), for the unrestricted space, the PFG NMR measurements may be represented by an effective diffusivity D_{eff} defined by the equation $\langle r^2(t)\rangle = 6D_{\mathrm{eff}} t$. In the dynamic MC simulations this is simply achieved by a completely random selection of the starting point of the diffusant.

Fig. 1 displays the results of our simulations. The conjuncture of the curves at $D/D_0 = N_{\mathrm{rem}}/N_0 = 0$ and 1, respectively, is easy to rationalize. For enabling comparison between different particle shapes, an effective particle radius has been introduced. For a three-dimensional lattice the effective particle radius is defined as three times the particle volume divided by its surface, $3V/S$, and coincides with the topological radius for spheres and half of the edge length for cubes. Considering the two terms of Eq. (2), the simulation parameter $\alpha R/5D_0$ is easily identified as the ratio of the time constants which would result in the limiting cases of diffusion- and barrier-limited exchange, respectively. Obviously, for each individual curve, time starts on top right and tends to infinity on bottom left. This means that for $N_{\mathrm{rem}}/N_0 = 1$ (top right) a negligibly small number of molecules has experienced the restriction by the surface so that their mean square displacement is still as if observed in the unrestricted space. By contrast, on bottom left, sufficiently large time has to have elapsed so that the displacements in the unrestricted space would have dramatically exceeded those of the molecules still within the crystal (since those are clearly limited by the crystal size). Let us now consider a certain fraction N_{rem}/N_0 between 0 and 1. As expected, the corresponding values D/D_0 are the small-

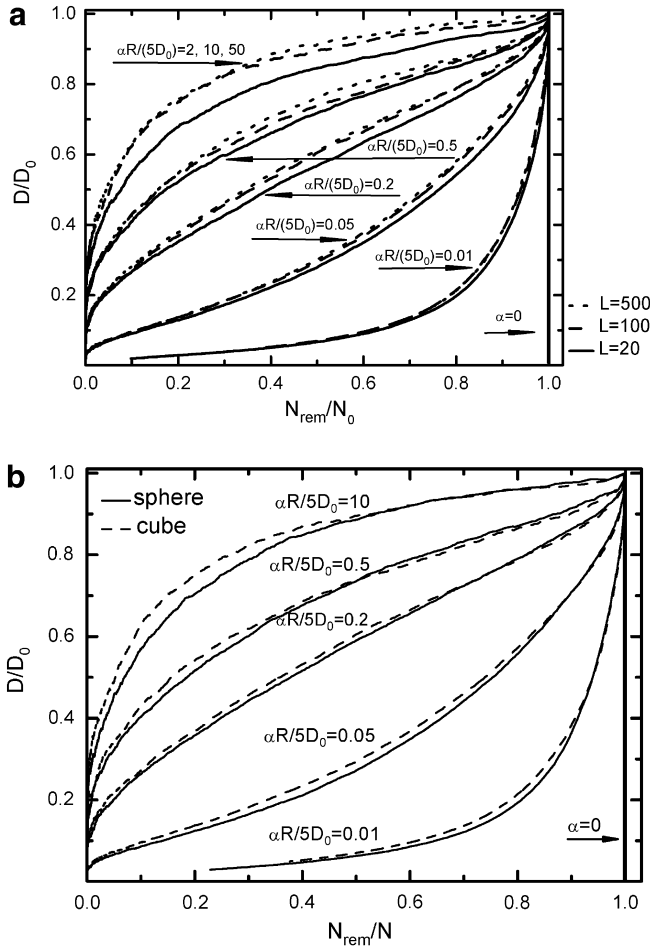

Fig. 1. Results of dynamic Monte Carlo simulations, correlating the intracrystalline mean square displacement normalized with respect to those in unrestricted space ($\langle r^2(t)\rangle_{\text{restricted}}/\langle r^2(t)\rangle_{\text{unrestr.}} = D(t)/D_0$) with the fraction $N_{\text{rem}}(t)/N_0$ of molecules which have not yet left their crystal, i.e., which give rise to the observed effective (restricted) diffusivity $D(t)$. The parameter $\alpha R/(5D_0)$ represents the ratio of the mean exchange times in the limiting cases of diffusion control ($R^2/(15D_0)$) and barrier control ($R/(3\alpha)$) for spherical particles. The quantity R in the representation is defined by the relation $3V/S$ between the particle volume (V) and surface (S), which coincides with the particle radius R in the case of spherical particles and half of the edge length for cubes. (a) The figure serves as a consistency check to demonstrate that the derived values converge to a well-defined limiting curve for sufficiently large values of L (corresponding to sufficiently small simulation step lengths) and, comprising the relations for cubic and spherical particles and (b) confirms that the obtained relations are only slightly affected by the particle shape.

er, the smaller the surface permeabilities (i.e. the stronger the surface barriers) are. Stronger surface barriers imply much longer molecular exchange times so that the molecules still remaining within the crystal have experienced restriction in a much more pronounced way than they would have (at the same level of exchange) with smaller surface resistances.

Fig. 1a provides a comparison of the simulation results for a cubic crystal. It demonstrates that for a sufficiently fine fragmentation, the system size in terms of the step length ($L = 20$, 100 and 500) is eventually found to be of no relevance for the result.

Fig. 1b represents the results of simulations performed with model crystals of different shape, namely with spherical particles and with cubes. The representations reflect the well-known fact [9] that the particle shape is of minor influence on the exchange behaviour. Most importantly, the separation between the curves for different parameters $\alpha R/5D_0$ is most pronounced in the medium range, i.e. for comparable transport resistances by intracrystalline diffusion and surface barriers. In the limiting cases where one of the two mechanisms is dominating, a variation of their intensity remains essentially invisible. Hence, if the simulation data are compared with experimental results, the range of highest sensitivity is that of comparable influence of intracrystalline diffusion and surface barriers. It was this range, where the conventional tracer desorption technique failed to provide reliable information about surface permeabilities. In the concluding section, the new option of applying PFG NMR will be illustrated by considering the transport behaviour of methane in a zeolite of structure type LTA [1], which, as a molecular sieve for hydrocarbon separation and detergent additive, is among the technologically most important zeolites.

3. Experimental

The zeolite material applied in these studies has been prepared following the classical Charnell method as described in [22,23]. The zeolite crystals are approximately cubes with average edge length of 5 and 35 μm, respectively. For the preparation of the PFG NMR samples, the zeolite material was introduced into sample tubes of 7.5 mm outer diameter, to a filling height of 10 mm. Under continuous evacuation, these tubes were heated at a rate of 10 K h^{-1} to 673 K. After keeping them at this temperature for about 12 h under continued evacuation and cooling down to the temperature of liquid nitrogen, a well-defined amount of methane (48 mg of methane per gram zeolite, corresponding to a loading of 5 molecules per cavity (“α cage” [1,22] of the internal pore structure)) was contained within the tubes. Finally, the samples were sealed.

The diffusion measurements were carried out using the home-built PFG NMR spectrometer FEGRIS 400 NT, operating at a ^{1}H resonance frequency of 400 MHz [24] with field gradient pulse amplitudes up to 35 Tm^{-1}. In order to decrease the disturbing influence of internal magnetic field inhomogeneities, the 13-interval bi-polar PFG NMR pulse sequence was used [25,26]. Generally, the diffusion measurements were performed by measuring the attenuation of the PFG NMR spin-echo signal ψ for a variable amplitude g of the field gradient pulses. For unrestricted, isotropic diffusion one has [25,26]

$$\psi = \exp\{-\gamma^2 g^2 (2\delta)^2 D(\Delta - \tau/2 - \delta/6)\} \tag{7}$$

where Δ denotes the separation of two field gradient pulses of equal polarity, and δ and τ stand for the width of the pulses and their separation in a (bipolar) pair. In general,

Δ can be chosen to notably exceed δ and τ. In such cases, the mean molecular displacements during the application of the bipolar pulse pairs are negligibly small in comparison with those during the time interval Δ between the two pairs. Hence, following the so-called narrow-pulse approximation of conventional PFG NMR [27,28], the time interval Δ may be simply interpreted as the observation time of the experiment (the "diffusion time"). Obviously, in cases where this approximation is not fulfilled anymore, the expression $(\Delta - \tau/2 - \delta/6)$ assumes the position of the genuine observation time. Therefore, we refer to it as an effective observation time, having in mind that for sufficiently large values of Δ this distinction is anyway of no relevance.

4. Results and discussion

Fig. 2a represents the set of attenuation plots of the PFG NMR spin-echo experiment attained with methane in zeolite NaCaA with a mean crystallite size of 5 μm for different observation times at 25 °C. The plots reflect the typical two-phase behaviour [29] implied for the application of the NMR tracer desorption technique [11,20], namely a first steep decay brought about by those molecules which, during the given observation time, have exchanged their positions between different crystallites. The second decay corresponds to those molecules which remain confined to the interior of one crystal. The distinction between these two constituents—and hence the determination of the fraction of molecules which, after the given observation time, have left their crystallites—is the easier, the more the intracrystalline diffusivity is exceeded by long-range diffusion. Recollecting that the long-range diffusivity may be represented as the product of the relative amount of molecules in the intercrystalline space and their diffusivity [7,11,30,31], we may expect the long-range diffusivities to be the larger the less favourably the guest molecules are adsorbed, i.e. the larger the external gas pressure has to be in order to maintain a certain guest concentration in the host system. Therefore, owing to is relatively low adsorption affinity, methane was intentionally chosen as a guest molecule to guarantee sufficiently high long-range diffusivities. The vast difference in the respective slopes in the attenuation plots of Fig. 2a fully complies with this expectation.

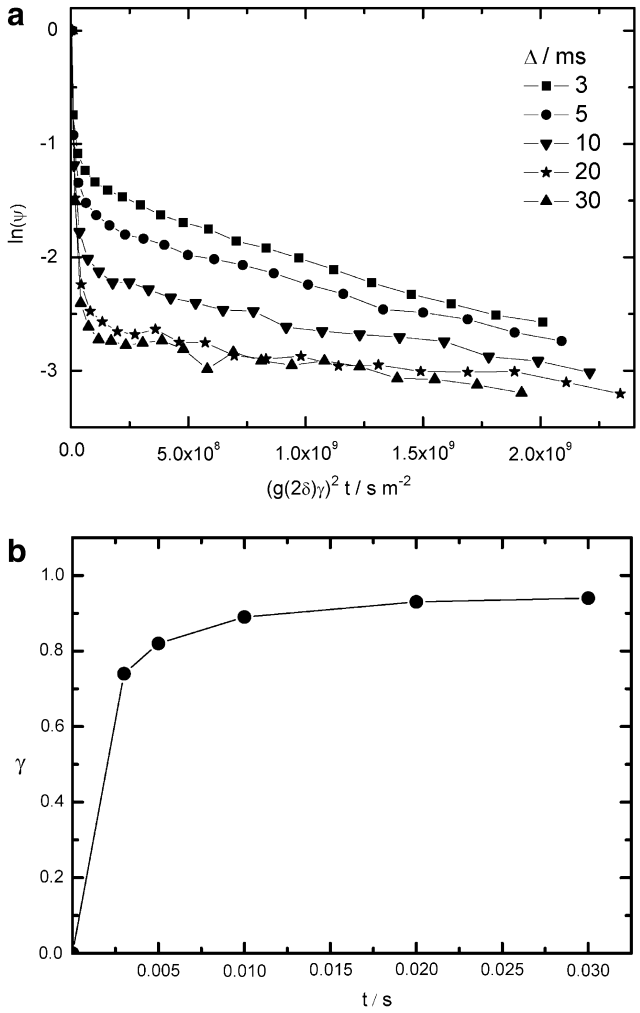

Fig. 2. Plots of the PFG NMR spin echo attenuation for different observation times (a) and the resulting PFG NMR tracer desorption curve (b) for methane in zeolite NaCaA crystals with average edge length of ca. 5 μm at 25 °C.

Fig. 2b displays the relative contribution of the second, less steep decay to the overall attenuation curve as a function of the effective observation time Δ. This curve is nothing else than the NMR tracer desorption curve $\gamma(t) = 1 - N_{\mathrm{rem}}(t)/N_0$. Application of Eq. (1) yields a mean molecular exchange time of $\tau_{\mathrm{ex}} = 9.1 \pm 1.8$ ms.

Application of Eq. (7) to the second, less steep decay yields an effective coefficient of intracrystalline diffusion, $D(t)$. It is defined by the Einstein relation (Eq. (4)), where the averaging procedure includes all molecules which, during the total observation time, have remained in one and the same crystal. Fig. 3 displays the resulting diffusivities as a function of the effective observation time. As a first-order approximation, i.e. for sufficiently short observation times, for diffusants subject to spherical confinement the effective diffusivities may be shown to obey the relation [20,21,32]

$$D(t) \approx D_0 - f\frac{D_0}{3R}\left(\frac{D_0 t}{\pi}\right)^{1/2} \tag{8}$$

with the numerical factor $f = 4$ for confinement by reflecting walls, and with $f = 2$ for absorbing walls. The time dependence of the effective coefficient of intracrystalline diffusion D of methane obtained for the 35 μm crystals was fitted by Eq. (8) (see Fig. 3). The resulting values of $D_0 = (1.4 \pm 0.3) \times 10^{-9}$ m^2 s^{-1} for the intracrystalline diffusivity, $f = 1.8 \pm 0.2$ for the numerical factor and $R = 15 \pm 3$ μm for the effective particle radius were found to be in reasonable agreement with previous experimental data [33] and the real size of the zeolite crystals,

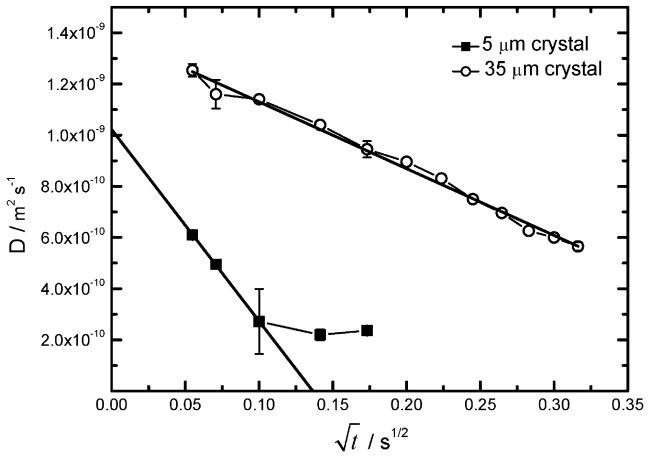

Fig. 3. Effective intracrystalline diffusivity of methane in NaCaA at 25 °C as resulting from the slope of that branch of the spin-echo attenuation plots (Fig. 2a) which corresponds to those molecules inside a crystallites which remain captured within these crystallites during the total observation time (second, less steep part in Fig. 2a).

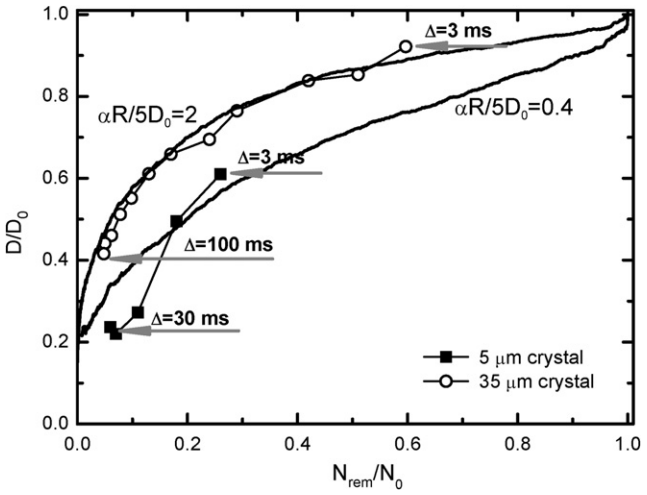

Fig. 4. Correlation plot of restricted diffusion (D/D_0) and tracer desorption (N_{rem}/N_0). Visual comparison of the experimental data obtained for methane in zeolite NaCaA with the corresponding theoretical curves obtained by dynamic Monte Carlo simulations (Fig. 1b for cubic crystals) gives the value of the parameter $\alpha R/5D_0$. The theoretical curves with $\alpha R/5D_0 = 0.4$ (for the 5 μm crystal) and $\alpha R/5D_0 = 2$ (for the 35 μm crystal) are found to provide the best fits to the experimental data.

respectively. The value of $f = 1.8$ approaches the theoretical value $f = 2$ for absorbing walls which with $p_{inter}D_{inter} \approx 6 \times 10^{-8}\ m^2\ s^{-1} \gg D_0$ has in fact to be expected in the given case.

The approximation by Eq. (8) is only applicable, however, if the root mean-square displacement of the molecules during observation time is much smaller than the mean size of the particles, i.e. if $\langle r^2(\Delta)\rangle^{1/2} \ll R$. Since the effective observation time is limited by the experimental conditions, this inequality is poorly realized for the smaller crystals of 5 μm, and the extrapolation may lead to substantial uncertainties. It is shown by Fig. 3 that in the given case, for the 5 μm crystals, the extrapolation of $D(t^{1/2})$ towards zero observation time leads to an intracrystalline diffusivity $D_0 = (1 \pm 0.4) \times 10^{-9}\ m^2\ s^{-1}$. Though being still in reasonable agreement with the data for the bigger crystals, this value is really of lower precision. It should be noted that there is neither need nor reason to expect coincidence of the correct values of the diffusivities. The inevitable differences in sample loading and in the real structure of the different zeolite specimens are known to readily lead to differences in the respective diffusivities [34].

Fig. 4 combines the two sets of experimental data displayed in Figs. 2b and 3, namely the relative numbers of molecules still remaining in one and the same crystal (abscissa) and their root mean square displacements (or their effective diffusivities) in relation to the corresponding values for unrestricted motion (ordinate), in the correlation scheme developed in the theoretical section. Direct comparison with the theoretical curves yields best agreement with the parameters $\alpha R/(5D_0) \approx 0.4 \pm 0.25$ and $\approx 2 \pm 0.8$ for the zeolite crystals of 5 and 35 μm edge length, respectively. With the respective crystal radii $R = 2.5$ and 17.5 μm and diffusivities $D_0 = (1 \pm 0.4) \times 10^{-9}$ and $D_0 = (1.4 \pm 0.3) \times 10^{-9}\ m^2\ s^{-1}$, this leads to surface permeabilities of $\alpha = (0.8 \pm 0.5) \times 10^{-3}$ and $\alpha = 0.78 \pm 0.3 \times 10^{-3}\ ms^{-1}$, respectively.

As to our knowledge, these values represent the first zeolite surface permeabilities ever obtained on the basis of direct experimental evidence. The fact that for different crystal sizes essentially identical surface resistances result, might be taken as an indication that—like the intracrystalline diffusivity—the surface resistance is a characteristic quantity of a given zeolite host–guest system. Having in mind, however, that today even the intracrystalline zeolitic diffusivity is found to be notably affected by deviations from a genuine intracrystalline porous structure [1,34], one should expect that similar effects may also occur with the much more unstable crystal boundary. Though, clearly, the ongoing systematic research of surface permeabilities has to provide a final answer, for the time being it cannot be excluded that the agreement in the surface permeabilities presently observed for two different specimens is only fortuitous.

Most interestingly, formal application of the values obtained and used in this study for the tracer exchange time ($\tau_{ex} = 9.1 \pm 1.8$ ms), the intracrystalline diffusivity ($D_0 = (1 \pm 0.4) \times 10^{-9}\ m^2\ s^{-1}$) and the mean crystal radius ($R = 2.5$ μm) to Eq. (2) yields a surface permeability of $\alpha = (0.1 \pm 0.02) \times 10^{-3}\ ms^{-1}$ which is by a factor of about 8 smaller than the value obtained by the novel method. Though, on the one hand, this comparison shows that estimates by the two methods yield results which do not differ by more than one order of magnitude, we take it again as an amber light not to overestimate the benefit of Eq. (2) for the quantitation of surface barriers. It is obvious that already a small fraction of particle agglomerates (which are inevitably met on studying such crystal powders) or of crystals with extremely high surface resistances may lead to very large (up to essentially infinite) exchange times. In

fact, the representation of Fig. 2, showing the relevant data points of the NMR tracer exchange curve, suggests such a tendency, since the rate of exchange is dramatically slowed down for fractional exchange above $\gamma \sim 0.8$. Therefore, if one is interested to explore the surface permeability of the vast majority of the crystals within the sample, one should have to discard this part of the NMR tracer exchange curve, which would result in much smaller values for the tracer exchange time τ_{ex}. As an immediate consequence, with a given value for the first term on the right hand side of Eq. (2), the magnitude of the second term would decrease (corresponding to the expected increase in the magnitude of the surface permeability α) and, eventually, the magnitudes of the terms get so closely together so that their uncertainties exclude the reliable determination of the surface permeability.

The novel method is based on an analysis which is insensitive to the pitfalls of such a limiting behaviour. Moreover, it takes account of the information provided by each individual point of the NMR tracer exchange curve rather than only of its first moment. The uncertainty of the determined permeabilities is typically on the order of a factor of 2 and most likely caused by the fact that the real systems studied notably deviate from the simplifying suppositions so far made in our simulations with respect to particle size and surface permeability, namely the absence of any dispersion. Future work has to comprise therefore efforts to approach the ideal systems considered in the simulations in the experimental reality and to extend the simulations to situations which allow an estimate of the influence of size and permeability dispersion on the analysis of the experimental data deduced from realistic systems.

5. Conclusions

Nanoporous solids with particle diameters in the range of micrometers are key to modern technologies of matter conversion and separation. The performance of most of these processes may be controlled by the permeability of the surface of these particles. This is in particular true since, during their industrial use, depositions of by-products on their outer surface or structural collapse close to their surfaces establish, or tend to enhance already existing, surface resistances. As a non-invasive technique and operating on the scale of micrometers which is particularly relevant for such systems, PFG (PGSE) NMR is ideally suited for quantitating such possible transport resistances on the particle surface.

We propose a new method to determine the intensity of such surface resistances. It is based on a special analysis of the so-called NMR tracer desorption experiment, in which the normalized effective diffusivities of the molecules that after a given time have not yet left their particles are plotted as a function of their fraction related to the molecules initially in a particle. These correlation curves are found to dramatically depend on the surface permeability. This is in particular true for the range where the transport resistances due to intraparticle (''intracrystalline'') diffusion and surface barriers are comparable. It is this range where the conventional method of simply comparing the molecular mean exchange time with its estimate on the basis of the intracrystalline diffusivity becomes questionable, as a consequence of the uncertainty in the primary quantities inherent to this method.

The proposed procedure is complementary to the short-time approach introduced by Mitra and Sen for quantitating the influence of internal walls on the PFG NMR data. In fact, it is only the upper (and, hence, right) part of our representation which is considered in their formalism, since deviations of $D(t)$ from D_0 are to be considered as small perturbations. Moreover, the present access allows covering the total spectrum of permeabilities between zero and infinity, while in the analytical solution one of the limiting cases of ideally reflecting walls (permeability zero) or absorbing walls is considered. In our context, the latter case refers to an infinite permeability, in conjunction with sufficiently fast diffusion in the external space. For covering the total exchange process and hence a time scale from zero to essentially infinity, we have to pay with being unable to provide an analytical solution.

Analysing the NMR tracer desorption curves of methane adsorbed on zeolite crystallites of type NaCaA, we have been able to deduce unprecedented information about the surface permeability of crystals in their as-synthesized state. Most remarkably, already without any further exposure of the crystallites, their surface is found to exert a finite transport resistance on molecular exchange which is not negligibly small in comparison with that due to intracrystalline diffusion.

Though the method has been introduced in particular for a better exploration of the internal dynamics in beds of microscopically small nanoporous particles, its application should be feasible for all aggregations of compartments (including cell tissues) [35,36] if the molecules, once they have left one of these compartments, are able to travel along sufficiently large paths so that their contribution to the NMR spin echo may be unambiguously separated by the PFG NMR experiments.

Acknowledgments

Financial support by the Deutsche Forschungsgemeinschaft, Fonds der Chemischen Industrie and the EU Marie Curie programme INDENS are gratefully acknowledged. Acknowledgment is also made by S.V. to the Donors of the American Chemical Society Petroleum Research Fund for support of this research. We are obliged to one of the referees for valuable suggestions and stimulating criticism.

References

[1] C. Baerlocher, W.M. Meier, D.H. Olson, Atlas of Zeolite Framework Types, Elsevier, Amsterdam, 2001.
[2] D.M. Ruthven, S. Farooq, K.S. Knaebel, Pressure Swing Adsorption, VHS, New York, 1994.

[3] J. Weitkamp, L. Puppe, Catalysis and Zeolites, Springer, Berlin/Heidelberg, 1999.
[4] P.T. Callaghan, Principles of Nuclear Magnetic Resonance Microscopy, Clarendon Press, Oxford, 1991.
[5] R. Kimmich, NMR Tomography, Diffusometry, Relaxometry, Springer, Berlin, 1997.
[6] J. Kärger, W. Heink, The propagator representation of molecular transport in microporous crystallites, J. Magn. Reson. 51 (1983) 1–7.
[7] J. Kärger, S. Vasenkov, Quantitation of diffusion in zeolite catalysts, Micropor. Mesopor. Mater. 85 (3) (2005) 195–206.
[8] J. Kärger, M. Kocirik, A. Zikanova, Molecular transport through assemblages of microporous particles, J. Colloid Interface Sci. 84 (1) (1981) 240–249.
[9] J. Kärger, D.M. Ruthven, Diffusion in Zeolites, Wiley, New York, 1992.
[10] J. Kärger, A study of fast tracer desorption in molecular sieve crystals, AIChE J. 28 (3) (1982) 417–422.
[11] J. Kärger, H. Pfeifer, W. Heink, Principles and application of self-diffusion measurements by nuclear magnetic resonance, Adv. Magn. Res. 12 (1988) 1–89.
[12] M. Goddard, D.M. Ruthven, Sorption and diffusion of C8 aromatic hydrocarbons in faujasite type zeolites III. Self-diffusivities by tracer exchange, Zeolites 6 (1986) 445–448.
[13] J. Kärger, W. Heink, H. Pfeifer, M. Rauscher, J. Hoffmann, NMR evidence for the existence of surface barriers on zeolite crystallites, Zeolites 2 (1982) 275–278.
[14] R.M. Barrer, Diffusion and Flow in: Porous Zeolite, Carbon or Ceramic Media, in: S.I. Gregg, K.S.W. Sing, H.F. Stoeckli (Eds.), Characterization of Porous Solids, Society of Chemical Industry, London, 1979, pp. 155–172.
[15] J. Kärger, M. Bülow, V.I. Ulin, A.M. Voloshchuk, P.P. Zolotarev, M. Kocirik, A. Zikanova, On the importance of dimension variation in determining the limiting steps in adsorption kinetics, J. Chem. Technol. Biotechnol. 32 (1982) 376–381.
[16] M. Kocirik, A. Zikanova, The analysis of the adsorption kinetics in materials with polydisperse pore structure, Ind. Eng. Chem. Fundam. 13 (4) (1975) 347–350.
[17] J. Crank, The Mathematics of Diffusion, Clarendon Press, Oxford, 1975.
[18] O.K. Dudko, A.M. Berezhkovskii, G.H. Weiss, Diffusion in the presence of periodically spaced permeable membranes, J. Chem. Phys. 121 (22) (2004) 11283–11288.
[19] J.E. Tanner, Transient diffusion in a system partitioned by permeable barriers. Application to NMR measurements with a pulsed field gradient, J. Chem. Phys. 69 (4) (1978) 1748–1754.
[20] O. Geier, R.Q. Snurr, F. Stallmach, J. Kärger, Boundary effects of molecular diffusion in nanoporous materials: A pulsed field gradient nuclear magnetic resonance study, J. Chem. Phys. 120 (1) (2004) 367–373.
[21] P.P. Mitra, P.N. Sen, L.M. Schwartz, Short-time behaviour of the diffusion coefficient as a geometrical probe of porous media, Phys. Rev. B 47 (1993) 8565–8574.
[22] J.F. Charnell, Gel growth of large crystals of sodium A and sodium X zeolites, J. Cryst. Growth 8 (3) (1971) 291–294.
[23] X. Yang, D. Albrecht, J. Caro, Revision of Charnell's procedure towards the synthesis of large and uniform crystals of zeolites A and X, Micropor. Mesopor. Mater. 90 (1-3) (2005) 53–61.
[24] P. Galvosas, F. Stallmach, G. Seiffert, J. Kärger, U. Kaess, G. Majer, Generation and application of ultra-high-intensity magnetic field gradient pulses for NMR spectroscopy, J. Magn. Reson. 151 (2) (2001) 260–268.
[25] P. Galvosas, F. Stallmach, J. Kärger, Background gradient suppression in stimulated echo NMR diffusion studies using magic pulsed field gradient ratios, J. Magn. Reson. 166 (2004) 164–173.
[26] R.M. Cotts, M.J.R. Hoch, T. Sun, J.T. Markert, Pulsed field gradient stimulated echo methods for improved NMR diffusion measurements in heterogeneous systems, J. Magn. Reson. 83 (1989) 252–266.
[27] R.W. Mair, M.N. Sen, M.D. Hurlimann, S. Patz, D.G. Cory, R.L. Walsworth, The narrow pulse approximation and long length scale determination in xenon gas diffusion NMR studies of model porous media, J. Magn. Reson. 156 (2) (2002) 202–212.
[28] P.P. Mitra, B.I. Halperin, Effects of finite gradient-pulse widths in pulsed-field-gradient diffusion measurements, J. Magn. Reson. Series A 113 (1) (1995) 94–101.
[29] W. Price, Application of pulsed gradient spin-echo NMR diffusion measurements to solution dynamics and organizations, in: J. Kärger, F. Grinberg, P. Heitjans (Eds.), Diffusion Fundamentals, Leipziger Universitätsverlag, Leipzig, 2005, pp. 490–508.
[30] I. Ardelean, G. Farrher, C. Mattea, R. Kimmich, NMR study of the vapor phase contribution to diffusion in partially filled silica glasses with nanometer and micrometer pores, Magn. Reson. Imag. 23 (2) (2005) 285–289.
[31] S. Vasenkov, O. Geier, J. Kärger, Gas diffusion in zeolite beds: PFG NMR evidence for different tortuosity factors in the Knudsen and bulk regimes, Eur. Phys. J. E 12 (1) (2003) 35–38.
[32] P.P. Mitra, P.N. Sen, Effect of microgeometry and surface relaxation on NMR pulsed-field-gradient experiments: Simple pore geometries, Phys. Rev. B 45 (1992) 143–156.
[33] W. Heink, J. Kärger, H. Pfeifer, et al., Self-diffusion measurements of n-alkanes in zeolite NaCaA by pulsed-field gradient nuclear magnetic resonance, J. Chem. Soc. Faraday T 88 (1992) 515–519.
[34] H. Jobic, J. Kärger, C. Krause, S. Brandani, A. Gunadi, A. Methivier, G. Ehlers, B. Farago, W. Haeussler, D.M. Ruthven, Diffusivities of n-alkanes in 5A zeolite measured by neutron spin echo, pulsed-field gradient NMR, and zero length column techniques, Adsorption 11 (2005) 403–407.
[35] T. Adalsteinsson, W.F. Dong, M. Schönhoff, Diffusion of 77 000 g/mol dextran in submicron polyelectrolyte capsule dispersions measured using PFG-NMR, J. Phys. Chem. B 108 (2004) 20056–20063.
[36] C. Meier, W. Dreher, D. Leibfritz, Diffusion in compartmental systems. II. Diffusion-weighted measurements of rat brain tissue in vivo and postmortem at very large b-values, Magn. Reson. Med. 50 (3) (2003) 510–514.